# Methanol Adsorption on the $\beta$-$Ga_2O_3$ Surface with Oxygen Vacancies: Theoretical and Experimental Approach

**María M. Branda,*,† Sebastián E. Collins,‡ Norberto J. Castellani,† Miguel A. Baltanás,‡ and Adrian L. Bonivardi‡**

*Departamento de Física, Grupo de Materiales y Sistemas Catalíticos, Universidad Nacional del Sur, Av. Alem 1253, 8000, Bahía Blanca, Argentina, and Instituto de Desarrollo Tecnológico para la Industria Química (INTEC), Güemes 3450, S3000GLN Santa Fe, Argentina*

*Received: January 6, 2006; In Final Form: April 5, 2006*

Methanol adsorption on $\beta$-$Ga_2O_3$ surface has been studied by Fourier transform infrared spectroscopy (FTIR) and by means of density functional theory (DFT) cluster model calculations. Adsorption sites of tetrahedral and octahedral gallium ions with different numbers of oxygen vacancies have been compared. The electronic properties of the adsorbed molecules have been monitored by computing adsorption energies, optimized geometry parameters, overlap populations, atomic charges, and vibrational frequencies. The gallia−methanol interaction has different behaviors according to the local surface chemical composition. The calculations show that methanol can react in three different ways with the gallia surface giving rise to a nondissociative adsorption, a dissociative adsorption, and an oxidative decomposition. The surface without oxygen vacancies is very reactive and produces the methanol molecule decomposition. The molecule is nondissociatively adsorbed by means of a hydrogen bond between the alcoholic hydrogen atom and a surface oxygen atom and a bond between the alcoholic oxygen atom and a surface gallium atom. Two neighbor oxygen vacancies on tetrahedral gallium sites produce the dissociation of the methanol molecule and the formation of a bridge bond between two surface gallium atoms and the methoxy group.

## 1. Introduction

The on-board hydrogen production to feed proton exchange membrane fuel cells, for their use in mobile sources, is a hot topic in catalysis nowadays.[1] In this context, methanol is regarded as the most suitable election because it has a high hydrogen-to-carbon ratio and, in comparison with alkenes or higher alcohol reforming, methanol reforming shows lower selectivity to byproducts, such as carbon monoxide and methane.[2−5] Also, methanol has no C−C bonds, which reduces the risk of catalyst coking. Thus, steam reforming of methanol (SRM)—$CH_3OH + H_2O = 3H_2 + CO_2$[1,2,5]—is a promising process to generate hydrogen.

The use of Pd-based catalysts for SRM (among which palladium supported onto reducible oxide supports has shown the higher selectivity to carbon dioxide and activity to hydrogen) has been recently reported in the literature.[3,6,8] Particularly, Iwasa et al. reported that Pd supported over gallium sesquioxide ($Ga_2O_3$ or gallia) was a very active and selective material, with a selectivity to $CO_2$ higher than 95%.[6,7]

With the aim to understand the mechanism of the selective catalytic production of hydrogen over the Pd−$Ga_2O_3$ system, some of us have recently investigated the superficial intermediates during the methanol decomposition over pure $\beta$-$Ga_2O_3$ and Pd/$\beta$-$Ga_2O_3$ by means of temperature-programmed surface reaction experiments, followed by in situ Fourier transform infrared spectroscopy (FTIR).[9] In that way, it was determined that adsorbed methanol is dehydrogenated stepwise to methylenebisoxy ($H_2COO$) and to mono- and bidentate formate groups (m- and b-HCOO, respectively), Finally, CO and $CO_2$ are further produced by nonstoichiometric transformation of these formates, leading to the release of atomic hydrogen on the surface of the oxide, as detected by the Ga−H stretching infrared band, and surface anion vacancies. In the presence of Pd dispersed on the gallia surface the same mechanism was found, but the metal accelerates the dehydrogenation of $CH_3O$ species because it favors the recombination and desorption as $H_2$(g) of the hydrogen atoms released in the previous steps, which are transferred from gallia to the Pd surface. Therefore, it was concluded that the relevant carbonaceous species during the methanol dehydrogenation are bonded to the gallium oxide surface.

Gallium $\beta$-$Ga_2O_3$ oxide is normally an insulator, with a forbidden energy gap of 4.84 eV. However, it is generally an n-type semiconductor due to oxygen vacancies individually compensated by two electrons forming shallow donors.[10] It is monoclinic with space group $C2/m$ and with lattice parameters $a = 12.23$ Å, $b = 3.04$, $c = 5.80$, and $\beta = 103.7°$.[11] The lattice is composed of two types of gallium ions, located respectively in tetrahedral and octahedral coordination sites, and three kinds of oxygen ions. Two oxygen ions are in a 3-fold coordination while the third is in a tetrahedral coordination.[10]

$\beta$-$Ga_2O_3$ is chemically and thermally extremely stable. This oxide shows polymorphism, but at high temperatures only its $\beta$ form is stable, and this is preserved upon cooling.[12] Hajnal et al. studied the electronic band structure of $\beta$-$Ga_2O_3$ and the formation and properties of oxygen vacancies in the bulk. They found formation energy values ($E^{2+}_{vac}$) between 4.3 and 6.1 eV.[12]

There are no reports of theoretical calculations about the methanol adsorption on Gallia. However, calculations based on

* To whom all correspondence should be sent. E-mail: cabranda@criba.edu.ar.

† Universidad Nacional del Sur.

‡ Instituto de Desarrollo Tecnológico para la Industria Química.

10.1021/jp060118n CCC: $33.50 
Published on Web 05/28/2006

density functional theory on adsorption of methanol on aluminum oxide were done by Borck et al.[13] They calculate the molecular adsorption energy $E_{ads} = 1.03$ eV/molecule. These calculations indicate that methanol adsorbs chemically by donating electron charge from the methanol oxygen to the surface aluminum.[13]

Particularly, we judge it now appropriate to focus on the methanol interaction with the active sites in the $Ga_2O_3$ surface. So, this paper couples experimental results obtained following the methanol adsorption over a $\beta$-$Ga_2O_3$ polymorph by in situ FTIR, as well DFT models of this process over selected clusters of (100) $\beta$-$Ga_2O_3$.

## 2. Experimental Section

**2.1. FTIR Experiments.** $\beta$-$Ga_2O_3$ was obtained from $Ga(NO_3)_3 \cdot xH_2O$ (Strem Chemicals, 99.99% Ga). An ammonia ethanolic solution (50%v/v) was added to 7% gallium nitrate in ethanol. The precipitated gel was washed with ethanol at room temperature until no nitrate anions were detected in the washing solution by UV spectroscopy. Afterward, the gel was dried at 343 K (1 h) and next calcined at 823 (8 h) and 923 K (6 h), in air. The single crystallographic structure of the obtained gallium oxide was verified by X-ray difraction spectrometry, and the specific surface area ($S_g$) was measured by the BET isotherm ($LN_2$, 77 K).

In situ FTIR spectroscopy was performed with use of 30 mg of $\beta$-$Ga_2O_3$ ($S_g = 64$ m$^2$/g) pressed into a self-supporting wafer (diameter = 13 mm) at 5 t/cm$^2$. The wafers were placed into a Pyrex IR cell, with water-cooled NaCl windows, which was attached to a conventional high-vacuum system (base pressure $= 1.33 \times 10^{-4}$ Pa), equipped with a manifold for gas flow. Before the adsorption experiments were done, the sample was activated by flowing pure $O_2$ into the cell (100 cm$^3$/min) from 298 to 723 K (5 K/min) then the temperature was immediately lowered to 373 K under He flow (60 cm$^3$/min). This activation treatment produces a partial dehydroxylation and gallium surface sites with O-vacancies.[14]

Methanol (Carlo Erba RPE, 99.9%) was purified by a series of freeze−thaw cycles under vacuum to remove dissolved gases and stored at 298 K in a glass bulb attached to the manifold. Then, methanol vapor was allowed into a small section of the manifold (which featured a sampling loop), and subsequently swept from the loop by flowing He (60 cm$^3$/min) and admitted into the IR cell, at 373 K. After methanol adsorption on the oxide sample, the cell was purged for 30 min by flowing He (60 cm$^3$/min).

The adsorption process was monitored by infrared spectroscopy by using a Shimadzu 8210 FTIR spectrometer equipped with a DLATGS detector (4 cm$^{-1}$ resolution, 100 scans).

Oxygen ($O_2$, AGA Research grade 99.996%) was passed through a molecular sieve (3 Å Fisher) and an Ascarite trap, to remove water and $CO_2$. Hellium (He, AGA UHP 99.999%) was further purified prior to use with use of molecular sieve (3 Å Fisher) and $MnO/Al_2O_3$ cartridges, to remove water and oxygen impurities.

**2.2. Computational Method.** Molecular orbital calculations were carried out in a model system comprised of a methanol molecule adsorbed on a defective (100) face of $\beta$-$Ga_2O_3$, which was represented by a cluster with suitable symmetry.

The $\beta$ gallia polymorph exhibits a $C2/m$ symmetry[11] with two different types of gallium atoms: one is centered in the middle of a tetrahedron ($Ga^{IV}$) and the other is centered in the middle of an octahedron ($Ga^{VI}$). The (100) plane is the more frequent and stable surface produced upon cleavage of $\beta$-$Ga_2O_3$ and is the normal growth axis of single crystals.[15,16] This plane consists only of oxygen atoms.

To study the adsorption of methanol on the (100) plane of $\beta$-$Ga_2O_3$ different clusters were considered, in which the $Ga^{3+}$ ions were on tetrahedral (designed as T) and octahedral (designed as O) positions, and surrounded by a different number of surface oxygen vacancies.

For T with 0, 1, and 3 oxygen vacancies the clusters were $Ga_{14}O_{21}^{(0)}$, $Ga_9O_{13}^{(1+)}$, and $Ga_{12}O_{18}^{(0)}$, respectively (see Figures 2−4) and for O with 0, 1, 2, and 3 oxygen vacancies the clusters were $Ga_{13}O_{20}^{(1-)}$, $Ga_{13}O_{19}^{(1+)}$, $Ga_{13}O_{19}^{(1+)}$, and $Ga_{13}O_{20}^{(1-)}$, respectively (see Figures 5−8). The numbers within parentheses are the charges of the clusters.

The use of a cluster to represent the interaction of small molecules with an oxide is justified by the fact that normally a limited number of atoms of the substrate participate in the adsorption process. Establishing the validity of a local description is of great importance, as it facilitates modeling of the ubiquitous surface inhomogeneities and point defects, which are believed to be active sites for these interactions.[17−19] For such problems, the cluster model and a localized description are often significantly more convenient than large scale periodic supercell calculations. The so-called "cluster size effects" refer to the long-range interactions, absent in the cluster, but present in the semi-infinite and periodic system. The importance of these effects (finite Madelung potential, dangling bonds of final atoms, for example) has been reported for many oxides in the literature and different remedial methods have been proposed to work out the problem.[19,20] One of them consists of putting the cluster within an embedding of point charges, to simulate the bulk. Taking into account that the $\beta$-$Ga_2O_3$ has a moderately ionic character, a careful selection of these point charges is an important requirement. For that purpose, first the net atomic charges for a greater and nearly stoichiometric cluster ($Ga_{23}O_{34}^{(1+)}$) were calculated. From these results we obtained that the average net atomic charges for Ga and O atoms are +0.75 e and −0.50 e, respectively. Afterward, using these values of charges for the embedding (∼250 point charges), we found that the adsorption energy ($E_{ads}$) for methanol on the T3 and O1 clusters (see Figures 4 and 6) changes only by ∼0.1 eV with respect to the situation without embedding. Considering the consistency between both series of results, we proceed to perform the rest of the calculations only with nonembedded clusters. Moreover, to obtain minimally charged clusters, the ones used here have the main bulk stoichiometry.

Density Functional Theory (DFT) quantum-mechanical calculations were carried out by using the gradient corrected Becke's three parameters hybrid exchange functional, in combination with the correlation functional of Lee, Yang, and Parr (B3LYP).[21,22]

The oxide O atoms were described with a locally dense 6-31G basis set. In this basis set, d-type orbitals for the O atoms involved in the adsorption process were added. The Ga atoms were treated with a small core ECP (effective core potential). The Ga basis set was that originally derived by Hay and Wadt,[23] with the contraction scheme implemented in the Gaussian03 code (LANL2DZ).[24] The methanol molecule was treated at the all-electron level with use of the 6-31G** basis set.

The adsorption energies were computed as the difference between the sum of the energies of the separated fragments and the energy of the methanol/gallia system. The full counterpoise procedure was applied to correct the basis set superposition error (BSSE).[25] Due to the fact that this method is particularly suitable when the fragments do not undergo important modifications of

**TABLE 1: Energetics of Methanol Adsorption on Various Sites of the (100) $Ga_2O_3$ Surface**

| site[a] | adsorption mode | $\Delta E_{ads}$ (eV) (BSSE) |
|---|---|---|
| T0 | oxidative decomposition | −5.74 |
| T1 | nondissociative adsorption | −1.84 (−1.43) |
| T3 | dissociative adsorption | −6.23 |
| O0 | oxidative decomposition | −12.42 |
| O1 | nondissociative adsorption | −1.62 (−1.17) |
| O2 | nondissociative adsorption | −1.95 (−1.50) |
| O3 | nondissociative adsorption | −1.45 (−1.00) |

[a] T and O designate tetrahedral and octahedral gallium atom sites and the subindexes the number of oxygen vacancies. [b] The BSSE corrected adsorption energy is given in parentheses. Negative values correspond to exothermic adsorption processes.

their geometries after bond formation, the correction was applied only in some cases (see Table 1).

The methanol molecule was fully geometrically optimized. The oxide geometry data were taken from ref 11. Mostly, surface oxygen atoms were fixed. Nevertheless, if oxygen atoms were involved in the surface reaction, they were also included in the optimization. The geometry optimization process was performed by means of analytical gradients with no symmetry constraints. The overlap population and the net atom charges were calculated by using the Mülliken population analysis.[26]

The vibrational frequencies were computed by determining the second derivatives of the total energy with respect to the internal coordinates. With the present approach, the calculated stretching frequencies for the free methanol molecule are overestimated with respect to the experimental values by about 3%. Thus, a scaling factor of 0.97 was applied to all the computed frequencies.

All the calculations were performed with the Gaussian-03 program package.[24]

## 3. Results and Discussion

**3.1. The Adsorption of Methanol by FTIR Spectroscopy.** After the adsorption of methanol on the activated $\beta$-$Ga_2O_3$ sample at 373 K, the IR cell was swept with flowing He during 30 min to ensure that only strong bonded species were present on the surface of the oxide. The IR spectrum shown in Figure 1 indicates that methanol exposure at 373 K produces two spectroscopically traceable surface species: molecularly adsorbed, Lewis-bound, methanol ($CH_3OH_S$), and dissociatively adsorbed methoxy groups ($CH_3O$).[9,27−30]

The IR spectral features are similar to those reported by Busca et al.[27] after the adsorption of methanol over $\delta$-$Al_2O_3$, and can be assigned as follows. Figure 1a shows that in the high-frequency region (>3000 $cm^{-1}$) a broad band developed between 3500 and 3300 $cm^{-1}$, which is assigned to the $\upsilon$(OH) mode of molecularly adsorbed methanol. The negative band at approximately 3650 $cm^{-1}$ was formed during the methanol adsorption process due to the consumption of the hydroxyl groups of the gallia surface. Simultaneously, the increase of the surface concentration of methoxy species occurred along with the liberation of gaseous $H_2O$, as revealed by the roto-vibrational bands around 1600 $cm^{-1}$ (not showed).[9]

The C−H asymmetric stretching of the methyl group [$\upsilon_{as}(CH_3)$] gives a very weak band (shoulder) at 2990 $cm^{-1}$ for both $CH_3OH_S$ and $CH_3O$ species (Figure 1b). Again, the C−H asymmetric and symmetric deformation mode (Figure 1a) [$\delta_{as}(CH_3) = 1469$ $cm^{-1}$ and $\delta_s(CH_3) = 1451$ $cm^{-1}$, respectively], and their overtones (Figure 1b) [$2\delta_{as}(CH_3) = 2925$ $cm^{-1}$ and $2\delta_s(CH_3) = 2859$ $cm^{-1}$], cannot allow any discrimination between molecularly adsorbed methanol or methoxy species.

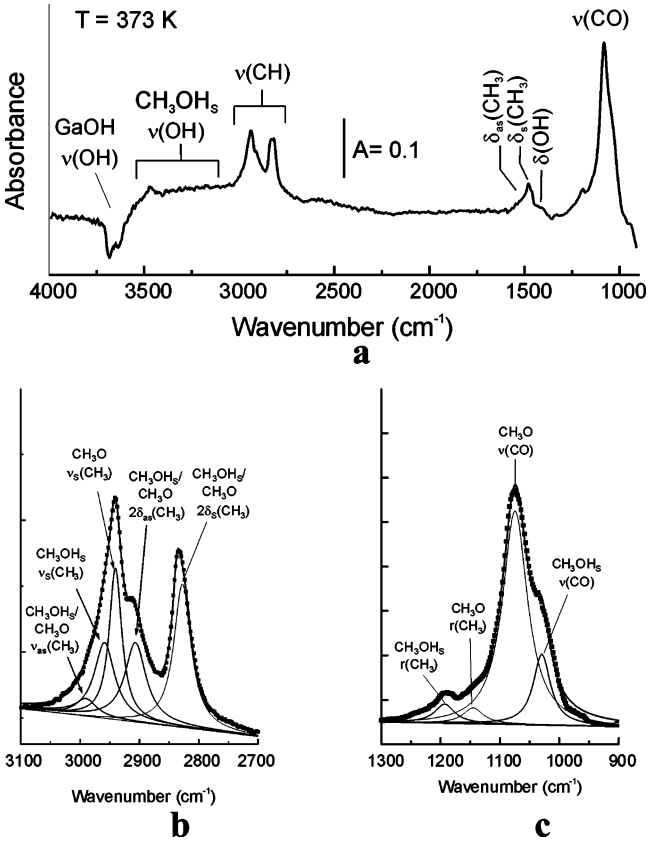


**Figure 1.** Infrared spectrum of adsorbed methanol at 373 K on activated $\beta$-$Ga_2O_3$ after flowing He (60 $cm^3$/min, 30 min).

Nevertheless, the peak centered at 2960 $cm^{-1}$ in Figure 1b is the result of two solved signals at 2958 and 2940 $cm^{-1}$ assigned to the C−H symmetric stretching of the $CH_3OH_S$ and $CH_3O$ surface species [$\upsilon_s(CH_3)$]. Furthermore, the weak IR signals of the C−H rocking modes [$\Gamma(CH_3)$] of methanol and methoxy groups are clearly discerned at 1183 and 1126 $cm^{-1}$ (Figure 1c), respectively, together with the C−O stretching vibration [$\upsilon$(CO)] at 1070 and 1030 $cm^{-1}$ for such different surface species.

We can then conclude that our infrared measurements verify the coexistence of both stable dissociated and nondissociated methanol groups over the surface of the $\beta$-$Ga_2O_3$ polymorph. The frequencies of the IR bands, which are typical of these species, are summarized later together with the theoretical results.

**3.2. The Methanol Interaction with Gallia Surface by DFT Calculations.** The optimized structures, detailing some of the relevant interatomic distances for all the studied adsorption sites, are shown in Figures 2−8. According to our theoretical results for the adsorption energies (see Table 1) and the final obtained geometries (Figures 2−8), the "adsorption modes" of the methanol molecule on the gallia substrate can be classified as (i) nondissociative adsorption (T1, O1, O2, and O3), (ii) dissociative adsorption (T3), and (iii) oxidative decomposition (T0 and O0). Negative values indicate exothermic adsorption processes.

The surfaces without oxygen vacancies, i.e., T0 and O0, are more reactive than the others. The methanol molecule oxidizes on these surfaces, forming $H_2CO$ in the first case and $CO_2$ and $H_2O$ in the second case. In both situations, surface hydroxyls are produced, too (see Figures 2 and 5). These molecules remain

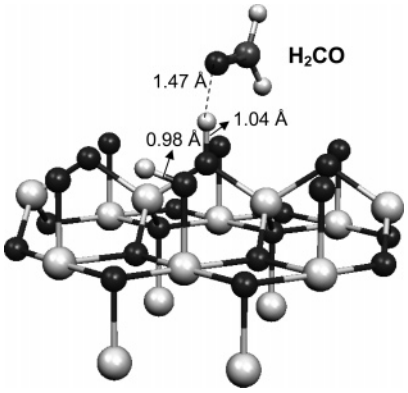


**Figure 2.** Optimal structure of a methanol molecule adsorbed on the T0 cluster, without oxygen vacancies. $H_2CO$ and surface hydroxyls are formed.

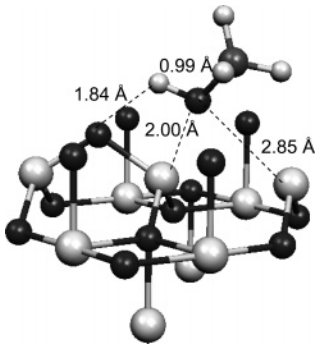


**Figure 3.** Optimal structure of a methanol molecule adsorbed on the T1 cluster, with 1 oxygen vacancy. A nondissociative adsorption occurs.

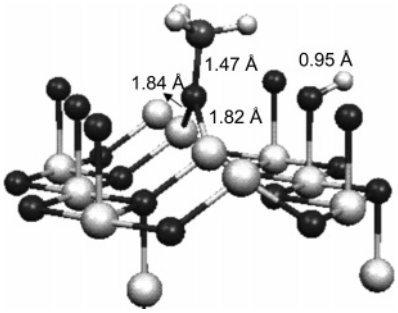


**Figure 4.** Optimal structure of a methanol molecule adsorbed on the T3 cluster, with 3 oxygen vacancies. The dissociation of methanol to methoxy is produced.

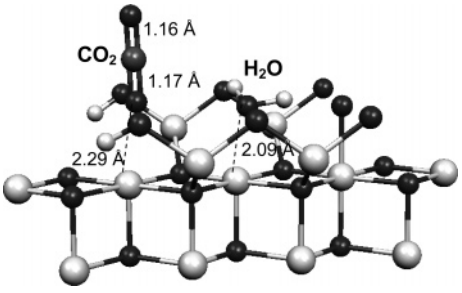


**Figure 5.** Optimal structure of a methanol molecule adsorbed on the O0 cluster, without oxygen vacancies. $CO_2$, $H_2O$, and surface hydroxyls are formed.

linked to the surface oxide. The $E_{ads}$ obtained for these sites are large: ~6 and ~12 eV, respectively. These results indicate that the (100) gallia surface without vacancies is very reactive, leading to the total decomposition of the methanol molecule.

On the other hand, it was found that the T3 site—with three oxygen vacancies on tetrahedral gallium atoms—is also quite

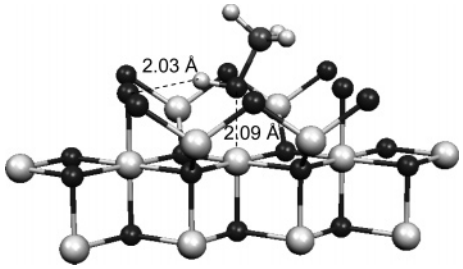


**Figure 6.** Optimal structure of a methanol molecule adsorbed on the O1 cluster, with 1 oxygen vacancy. A nondissociative adsorption occurs.

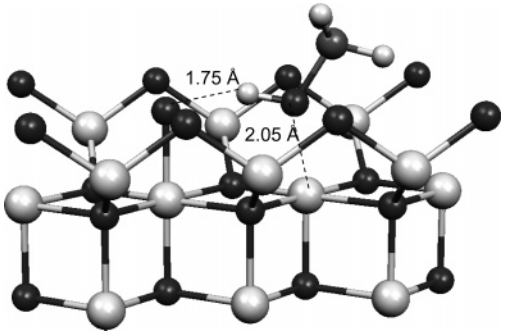


**Figure 7.** Optimal structure of a methanol molecule adsorbed on the O2 cluster, with 2 oxygen vacancies. A nondissociative adsorption occurs.

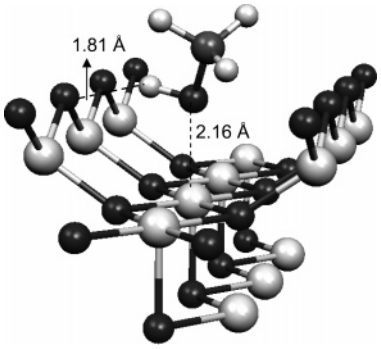


**Figure 8.** Optimal structure of a methanol molecule adsorbed on the O3 cluster, with 3 oxygen vacancies. A nondissociative adsorption occurs.

reactive, producing the dissociation of methanol to methoxy. The corresponding $E_{ads}$ is large, too (~6 eV), as in the case of the T0 and O0 sites. The adsorption energies when the methanol molecule is nondissociatively adsorbed are much lower, going from ~1.4 eV to ~1.9 eV (~1.0 eV to ~1.5 eV with the BSSE correction).

To compare these results with the IR experimental data, we will focus in this study only on the nondissociative (T1, O1, O2, and O3) and the dissociative (T3) adsorptions.

Table 2 shows selected geometrical parameters in the methanol−allia interaction after optimization. Regarding the different possibilities of the nondissociative adsorption, it can be observed that the $H_{alc}-O_s$ distance between the methanol molecule and the surface oxide is in the 1.7−2.0 Å interval. The process with the largest $E_{ads}$ corresponds to the shortest bond distance, in O2 (see Table 1 and Figure 7).

When the adsorption occurs nondissociatively the O−H alcoholic bond is lengthened, going from 0.96 Å for the free methanol molecule to 0.99−1.01 Å for the adsorbed molecule, thus indicating a weakening of this bond. On the other hand, the interatomic distance of the ($Ga-O_{alc}$) bond is always ~2 Å, similar to that of the ($Ga^{VI}-O_s$) oxide ionic bond. In addition,

**TABLE 2: Main Geometrical Parameters of Methanol Adsorbed on the (100) $Ga_2O_3$ Surface**

| | $d(O-H)_{alc}$ [Å] | $d(C-O)$ [Å] | ∠(COH) [deg] | $d(H_{alc}\cdots O_s)$ [Å] | $d(Ga\cdots O_{alc})$ [Å] | $d(H_{methyl}-O_s)$ [Å] |
|---|---|---|---|---|---|---|
| methanol | 0.96 | 1.42 | 107.9 | | | |
| T1 | 0.99 | 1.46 | 111.6 | 1.84 | 2.00 | 2.11 |
| T3 | 3.55 | 1.47 | − | 0.95 | 1.82/1.84 | 2.39 |
| O1 | 0.99 | 1.47 | 105.1 | 2.03 | 2.09 | 2.41/2.48 |
| O2 | 1.01 | 1.46 | 111.5 | 1.75 | 2.05 | 2.39 |
| O3 | 0.99 | 1.48 | 104.0 | 1.81 | 2.16 | 2.26/2.45 |

[a] Methanol intramolecular and methanol−surface interatomic distances ($d(O-H)/d(C-O)$ and $d(H_{alc}\cdots O_s)/d(Ga\cdots O_{alc})/d(H_{methyl}-O_s)$, respectively), and methanol ∠COH angle at equilibrium obtained after optimization. T and O designate tetrahedral and octahedral gallium atom sites and the subindexes the number of oxygen vacancies.

**TABLE 3: Overlap Populations for the Methanol Adsorption on Different Sites of the (100) $Ga_2O_3$ Surface[a]**

| | $(O-H)_{alc}$ | $(C-O)_{alc}$ | $(H_{alc}\cdots O_s)$ | $(Ga\cdots O_{alc})$ | $(H_{methyl}\cdots O_s)$ |
|---|---|---|---|---|---|
| methanol | 0.30 | 0.26 | | | |
| T1 | 0.28 | 0.19 | 0.04 | 0.12 | 0.02 |
| T3 | 0.00 | 0.18 | 0.29 | 0.16/0.13 | 0.02 |
| O1 | 0.26 | 0.20 | 0.05 | 0.11 | 0.00/0.00 |
| O2 | 0.24 | 0.19 | 0.07 | 0.13 | 0.01 |
| O3 | 0.25 | 0.20 | 0.05 | 0.11 | 0.03/0.00 |

[a] T and O designate tetrahedral and octahedral gallium atom sites and the subindexes the number of oxygen vacancies.

in these nondissociative adsorption cases, the $-CH_3$ group becomes linked to the oxide surface with a hydrogen bond of 2.1−2.5 Å (see Figures 3, 4, 6, 7, and 8) between a hydrogen methyl atom ($H_{methyl}$) and an oxygen atom of the substrate ($O_s$).

When methanol dissociates in T3, a strong (O−H) bond between the surface oxygen atom and the hydrogen atom coming from methanol is formed, with a typical bond distance for the hydroxyl group (0.95 Å). Two surface gallium atoms hold the methoxy group with a strong link, with a bond distance similar to the bulk $Ga^{IV}-O$ bond, ∼1.8 Å (see Figure 4).

For both adsorption processes, nondissociative and dissociative, the (C−O) bond of the methanol molecule, in the first case, and methoxy, in the second one, become stretched. This bond elongates from 1.42 Å for the free species to 1.46−1.51 Å for the adsorbed species, indicating also a weakening of this link.

In Table 3, the overlap population values for the same bonds considered in Table 2 are summarized. Notice that the $OP(H_{alc}-O_s)$ value (∼0.3) for the dissociated species is similar to the OP(H−O) one for the free methanol molecule, which indicates that this bond has covalent character. On the other hand, the $OP(H_{alc}-O_s)$ values for the nondissociative species go from 0.04 to 0.07, as would be expected for a hydrogen bond. In this case, we have different OP values depending on the link distances (see Table 2). With respect to the $OP(Ga-O_{alc})$ values, they are analogous to those for the $(Ga-O_s)$ bonds. Actually, the $OP(Ga-O_{alc})$ for T3, where the oxygen atom takes a bridge configuration between two gallium ions, is slightly larger than that in the nondissociated cases.

The last column of Table 3 shows that the $(H_{methyl}-O_s)$ bond has very small OP values in comparison with the $H_{alc}-O_s$ results, in agreement with an (expected) relatively weak hydrogen bond. Also notice that the interatomic distances are much longer in the last situation (see Table 2). Finally, the $OP(O-H)_{alc}$ and $OP(C-O)_{alc}$ values for the nondissociative methanol adsorption are smaller than those for the free molecule, in agreement with bond stretching, and the corresponding bond weakening.

Table 4 shows some of the calculated changes of the Mülliken net charges when the methanol molecule becomes linked to the different (100) gallia sites, vs the isolated species. These results

**TABLE 4: Difference between the Mülliken Atomic Charges When the Methanol Molecule is Linked with the (100) $Ga_2O_3$ Surface and the Isolated Species[a]**

| | $\Delta Q$(methanol) | $\Delta Q(H_{alc})$ | $\Delta Q(O_{alc})$ | $\Delta Q$(Ga) | $\Delta Q(O_s)$ |
|---|---|---|---|---|---|
| T1 | +0.23 | +0.12 | −0.08 | +0.19 | −0.15 |
| T3 | −0.13 | −0.02 | −0.33 | +0.45/+0.31 | −0.23 |
| O1 | +0.12 | +0.06 | −0.12 | +0.17 | −0.06 |
| O2 | +0.13 | +0.09 | −0.13 | +0.16 | −0.10 |
| O3 | +0.10 | +0.02 | −0.05 | +0.10 | −0.06 |

[a] T and O designate tetrahedral and octahedral gallium atom sites and the subindexes the number of oxygen vacancies.

**TABLE 5: Experimental and Calculated IR Frequencies Modes for the Free Methanol Molecule**

| vibrational mode | exptl ($cm^{-1}$) | calcd CIS ($cm^{-1}$) | calcd TRANS ($cm^{-1}$) |
|---|---|---|---|
| $\upsilon$(OH) | 3709 (R)<br>3681 (Q)<br>3664 (P) | 3757 | 3715 |
| $\upsilon_s(CH_3)$ | 2868 (R)<br>2844 (Q)<br>2826 (P) | 2921 | 2899 |
| $\upsilon_{as}(CH_3)$ | 3006<br>2973 | 2987<br>2977 | 3028<br>2943 |
| $\upsilon$(CO) | 1057 (R)<br>1032 (Q)<br>1014 (P) | 1034 | 1033 |
| $\delta$(OH) | 1345 | 1325 | 1342 |
| $\delta_s(CH_3)$ | 1453 | 1460 | 1456 |
| $\delta_{as}(CH_3)$ | 1474 | 1485<br>1454 | 1480<br>1463 |
| $\Gamma(CH_3)$ | | 1157 | 1143 |

indicate that the dissociated methanol takes a negative charge from the substrate. Conversely, the methanol molecule gives up electronic charge to the surface whenever it is not dissociated, thus becoming positively charged. In this way, and as we should expect, the substrate acts as an acid oxide in almost all cases. Although the $O_s$ also takes a negative charge, the charge lost by the gallium atoms is always larger. Looking at the charge changes of the hydrogen and oxygen atoms of the alcoholic −OH group, one observes that upon adsorption this bond has a higher polarization, the first atom resulting more positive and the latter more negative. The gallia atoms involved in the $CH_3$-OH−gallia interaction also undergo a charge modification when the gallium atom (linked to $O_{alc}$) becomes more positive whereas the $O_s$ atom (linked to either the tetrahedral, $Ga^{IV}$ or octahedral, $Ga^{VI}$ atoms) becomes more negative, respectively. Therefore, the −OH dipole of the methanol molecule couples electrostaticaly with a dipole residing on the gallia surface.

The (theoretical) IR active vibrational modes of the free methanol molecule (cis and trans configurations) were calculated and compared with the available experimental data (Table 5). The frequency values calculated from DFT total energy results are normally overestimated. To have a better set of results the values of this table have been renormalized by multiplying by

**TABLE 6: Selected Frequency Modes for Methanol Adsorbed on Different Sites of the (100) $Ga_2O_3$ Surface**

| | exptl | | methanol/gallia calcd ($cm^{-1}$), site = | | | | |
|---|---|---|---|---|---|---|---|
| vibrational mode | $CH_3O$ ($cm^{-1}$) | $CH_3OH_S$ ($cm^{-1}$) | $T_1$ | $T_3$ | $O_1$ | $O_2$ | $O_3$ |
| $\upsilon$(OH) | | 3275 | 3294 | 3862 ($O_sH$) | 3319 | 2926 | 3284 |
| $\upsilon_s(CH_3)$ | 2940 | 2958 | 2882 | 2995 | 3020 | 2996 | 2968 |
| $\upsilon_{as}(CH_3)$ | 2990 | 2990 | 3105 | 3092 | 3149 | 3102 | 3106 |
| | | | 3035 | 3114 | 3113 | 3084 | 3054 |
| $\upsilon$(CO) | 1070 | 1030 | 955 | 962 | 920 | 964 | 911 |
| $\delta$(OH) | | 1315 | 1337 | | | | |
| $\delta_s(CH_3)$ | 1451 | 1451 | 1411 | 1407 | 1432 | 1421 | 1500 |
| $\delta_{as}(CH_3)$ | 1469 | 1469 | 1416 | 1458 | 1456 | 1449 | 1474 |
| | | | 1455 | 1470 | 1466 | 1475 | 1462 |
| $\Gamma(CH_3)$ | 1140 | 1187 | 1137 | 1125 | 1141 | 1133 | 1166 |
| | | | | 1183 | 1156 | 1139 | 1146 |

a factor of 0.97. In this way a more successful comparison with experimental spectra can be attained. If this renormalization is later used for the methanol molecule in other chemical environments, the corrected vibrational frequencies can be compared with higher confidence with the corresponding (independent) experimental results.

Table 6 summarizes the experimental and calculated vibrational frequencies corresponding to the fundamental modes of the adsorbed methanol on the gallia surface. The latter were scaled down by using the abovementioned 0.97 renormalizing factor, for the nondissociative and the dissociative species as well. For the dissociated species, the stretching mode $\upsilon$(OH) actually corresponds to a surface hydroxyl: Ga−$O_s$H. Its frequency value (3862 $cm^{-1}$) is somewhat higher than the experimental one for isolated −OH (3746 $cm^{-1}$) (see refs 9 and 14). This difference could be explained by the presence of further coupling of the −OH groups with the neighbor atoms of the real (extended) surface.

Both the experimental and calculated results of $\upsilon$(OH) for the free (Table 5) and the adsorbed methanol molecule (Table 6) show a red shift of about 400 $cm^{-1}$, indicating a weakening of the OH bond once the adsorbate approaches the gallia surface. The calculated $\upsilon$(OH) for the nondissociatively adsorbed methanol molecule goes from ∼2930 to ∼3340 $cm^{-1}$. The frequency values corresponding to the T1, O1, and O3 sites (∼3300 $cm^{-1}$) are similar to the experimental ones. The value for methanol on the O2 site (∼2930 $cm^{-1}$) is compatible with an even weaker OH bond, which is in agreement with the more stretched oxygen−hydrogen bond shown in Figure 7 (see also Table 2).

Similar red shifts were found for the theoretical values of the $\upsilon$(CO) modes (∼70 to 120 $cm^{-1}$), which are dependent on the (CO) bond length. The experimental shift for this vibrational mode was almost negligible, though. The largest red shift, for the methanol adsorbed on the O3 site, is compatible with a weaker C−O bond and it is in agreement with a relevant stretching (0.06 Å) of the carbon−oxygen bond (see Table 2). Such a low C−O frequency was not observed in experiments. Nevertheless, it corresponds to the methanol nondissociative adsorption geometry with the lowest adsorption energy (see Table 1), on a—probably quite unlikely or sparsely populated—octahedral surface site with three oxygen vacancies. Hence, this type of adsorbed methanol would certainly not be detected in the IR spectra.

The calculated frequencies for the bending modes are in good agreement with the FTIR experimental values. Notice that, other than for the $\delta$(OH) mode, the measured symmetrical and antisymmetrical $\delta(CH_3)$ modes do not change significantly when the methanol adsorbs on gallia or, in other words, that the adsorption process barely perturbs the methyl group. The same occurs with the $\Gamma(CH_3)$ mode.

Notice that it can be seen that the symmetrical and antisymmetrical $\delta(CH_3)$ modes do not change significantly when the methanol adsorbs on gallia. The same property occurs with $\delta$-$(CH_3)$ modes.

## 4. Conclusions

The computational results allow us to conclude that the interaction of the methanol molecule with the gallia surface strongly depends on the local surface chemical environment. The $\beta$-$Ga_2O_3$ (100) surface without oxygen vacancies is very reactive and produces the oxidative decomposition of the methanol molecule. However, that molecule is nondissociatively adsorbed by means of two ionic bonds on the gallia surface with oxygen vacancies. A hydrogen bond between the alcoholic hydrogen atom and a surface oxygen atom and a bond between the alcoholic oxygen atom and a surface gallium atom are formed. This process occurs on tetrahedral and octahedral gallium sites with $E_{ads}$ from 1.0 to 1.5 eV. The O−H and C−O bonds are elongated and weakened after the adsorption process, and become more polarized. The nondissociative adsorption produces a charge transfer from the molecule to the substrate.

Two neighbor oxygen vacancies on tetrahedral gallium sites produce the dissociation of the methanol molecule and the formation of a bridge bond between two surface gallium atoms and the methoxy group.

The theoretical results are in good agreement with the formation of molecular adsorbed methanol and methoxy groups as detected by IR spectroscopic measuremtens on an activated sample of single phase $\beta$-gallia.

**Acknowledgment.** This work was supported by ANCyPT (PICT 13-07005, PICT 14-12369) and CONICET (PIP 5245).

## References and Notes

(1) Carrette, L.; Friedrich, K. A.; Stimming, U. *Fuel Cells* **2001**, *1*, 5.
(2) Rostrup-Nielsen, J. R. *Phys. Chem. Chem. Phys*. **2001**, *3*, 283.
(3) Agrell, J.; Hasselbo, K.; Jansson, K.; Järas, S. G.; Boutonnet, M. *Appl. Catal. A* **2001**, *211*, 239.
(4) Lindström, B.; Petterson, L. J. *J. Power Sources* **2003**, *118*, 71.
(5) Agrell, J.; Birgersson, H.; Boutonnet, M.; Melia'n-Cabrera, I.; Navarro, R. N.; García Fierro, J. L. *J. Catal*. **2003**, *219*, 389.
(6) Iwasa, N.; Mayanagi, T.; Ogawa, N.; Sakata, K.; Takezawa, N. *Catal. Lett*. **1998**, *54*, 119.
(7) Iwasa, N.; Mayanagi, T.; Nomura, W.; Arai, M.; Takezawa, N. *Appl. Catal. A* **2003**, *248*, 153.
(8) Liu, S.; Takahashi, K.; Ayabe, M. *Catal. Today* **2003**, *87*, 247.
(9) Collins, S. E.; Baltanás, M. A.; Bonivardi, A. L. *Appl. Catal. A* **2005**, *295*, 126−133.
(10) Binet, L.; Gourier, D.; Minot, C. *J. Solid State Chem.* **1994**, *113*, 420.
(11) Geller, S. *J. Chem. Phys.* **1960**, *33*, 676.
(12) Hajnal, Z.; Miró, J.; Kiss, G.; Réti, F.; Deák, P.; Herndon, R. C.; Kuperberg, J. M. *J. Appl. Phys.* **1999**, *86 N° 7*, 3792.
(13) Borck, Ø.; Schröder, E. *ATB Metall.* **2003**, *43*, 342.
(14) Collins, S. E.; Baltanás, M. A.; Bonivardi, A. L. *Langmuir* **2005**, *21*, 962.
(15) Kohl, D.; Ochs, Th.; Geyer, W.; Fleischer, M.; Meixner, H. *Sens. Actuators, B* **1999**, *59*, 140.
(16) Chase, A. B. *J. Am. Ceram. Soc.* **1964**, *47/9*, 470.
(17) Henry, C. R. *Surf. Sci. Rep*. **1998**, *31*, 231.
(18) Branda, M. M.; Ferullo, R. M.; Belelli, P. G.; Castellani, N. J. *Surf. Sci.* **2003**, *527* (Nos. 1−3), 89.
(19) Branda, M. M.; Di Valentin, C.; Pacchioni, G. *J. Phys. Chem. B* **2004**, *108*, 4752.
(20) Ferullo, R. M.; Castellani, N. J. *J. Mol. Catal. A*: *Chem.* **2004**, *221*, 155.
(21) Becke, A. D. *J. Chem. Phys*, **1993**, *98*, 5648.
(22) Lee, C.; Yang, W.; Parr, R. G. *Phys. Rev. B* **1988**, *37*, 785.
(23) Hay, P. J.; Wadt, W. R. *J. Chem. Phys.* **1985**, *82*, 299.

(24) Frisch, M. J.; et al. *Gaussian03*; Gaussian Inc.: Pittsburgh, PA, 1998.
(25) Boys, S. F.; Bernardi, F. *Mol. Phys.* **1970**, *19*, 553.
(26) Levine, I. N. *Quantum Chemistry*, 5th ed.; Prentice Hall: Upper Saddle River, NJ, 2000.
(27) Busca, G.; Rossi, P. F.; Lorenzelli, V.; Benaissa, M.; Travert, J.; Lavalley, J. C. *J. Phys. Chem.* **1985**, *89*, 5433.
(28) Busca, G. *Catal. Today* **1996**, *27*, 457.
(29) Burcham, L. J.; Badlani, M.; Wachs, I. E. *J. Catal.* **2001**, *203*, 104.
(30) Lavalley, J. C. *Catal. Today* **1996**, *27*, 377.